Middle-East Journal of Scientific Research 23 (10): 2484-2492, 2015
ISSN 1990-9233

DOI: 10.5829/idosi.mejsr.2015.23.10.95132

An Efficient Method for Retinal Hemorrages Detection in Fundus Images Using Anfis and Cross Section Profile Analysis

[1]P. Kumar and [2]L. Godlin Atlas

[1]Centre for Information Technology and Engineering,
M.S University, Tirunelveli, Tamilnadu, India
[2]Maria College of Engineering and Technology, Kanyakumari, Tamilnadu, India

Abstract: Automated techniques for eye diseases identification are very important in the ophthalmology field. Conventional techniques for the identification of retinal diseases are based on manual observation of the retinal components (optic disk, macula, vessels, etc.). This paper presents a new supervised method for hemorrhages detection in digital retinal images. This method uses a ANFIS scheme for pixel organization and computes a 5-D vector composed of gray-level and Cross Section Profie Analysis-based features for pixel representation. The method was evaluated on the publicly available DRIVE and STARE databases, widely used for this intention since they contain retinal images where the vascular structure has been precisely marked by experts. Its effectiveness and robustness with different image conditions, together with its simplicity and fast implementation, make this blood vessel segmentation proposal suitable for retinal image computer analyses such as automated screening for early diabetic retinopathy detection.

Key words : Diabetic Retinopathy · Hemorrage · Retinal Imaging · Telemedicine · Vessels Segmentation

INTRODUCTION

Recent advances in computer technology have enabled the progress of numerous types of Computer-Aided Medical Diagnosis - CAMD - over the years. Currently, medical image analysis is a research area that attracts a lot of concern from both scientists and physicians. Computerized medical imaging and analysis methods using multiple modalities have facilitated early diagnosis, treatment evaluation and therapeutic intervention in the clinical management of critical diseases [1]. DIABETIC retinopathy (DR) is the leading ophthalmic pathological cause of blindness among people of working age in developed countries. It is motivated by diabetes-mellitus complications and, although diabetes warmth does not necessarily involve vision impairment, about 2% of the patients affected by this disorder are blind and 10% undergo vision degradation after 15 years of diabetes, as a consequence of DR complications. The estimated prevalence of diabetes for all age groups worldwide was 2.8% in 2000 and 4.4% in 2030, meaning that the total number of diabetes patients is forecasted to rise from 171 million in 2000 to 366 million in 2030 [2]. The detection of hemorrhages is one of the important factors in the early diagnosis of diabetic retinopathy (DR). The existence of hemorrhages is generally used to diagnose DR or hypertensive retinopathy by using the classification scheme of Scheie.

Several automated techniques have been reported to quantify the changes in morphology of retinal vessels (width, tortuosity) indicative of retinal or cardiovascular diseases. Some of the techniques measure the vessel morphology as an average value representing the entire vessel network, e.g., average tortuosity [3]. However recently, vessel morphology measurement specific to arteries or veins was found to be associated with disease. For example, 'plus' disease in retinopathy of prematurity (ROP) may result in increase in arterial tortuosity relative to that of veins indicating the need for preventative treatment [4]. Arterial narrowing, venous dilatation and resulting decrease in artery-to- venous width ratio (AVR) may predict the future occurrence of a stroke event or a myocardial infarct [5]. Unfortunately, the detection of minute changes in vessel width or tortuosity specific to

Corresponding Author: L. Godlin Atlas, Maria College of Engineering and Technology, Kanyakumari, Tamilnadu, India.

arteries or veins may be difficult in a visual evaluation by an ophthalmologist or by a semi-automated method, which is laborious in clinical practice. Therefore, an automated identifica- tion and separation of individual vessel trees and the subsequent classification into arteries and veins is required for vessel specific morphology analysis [6].

Blood vessels appeared as networks of either deep red or orange-red filaments that originated within the optic disc and were of progressively diminishing width. Several approaches for extracting retinal image vessels have been developed which can be divided as; one consists of supervised classifier-based algorithms and the other utilizes tracking-based approaches. Supervised classifier-based algorithm usually comprise of two steps. First, a low-level algorithm produces segmentation of spatially connected regions. These candidate regions are then classified as vascular or non-vascular. The application of mathematical morphology and wavelet transform was investigated for identification of retinal blood vessels [7]. In a follow-up study, a two-dimensional Gabor wavelet was utilized to initially segment the retinal images.

A Bayesian classifier was then applied to classify extracted feature vectors as vascular or non-vascular. Tracking-based approaches utilize a profile model to incrementally step along and segment a vessel. Vessel tracking proceeded iteratively from the papilla, halting when the response to a one-dimensional matched filter fell below a given threshold. The tracking method was driven by a fuzzy model of a one-dimensional vessel profile [8]. One drawback to these approaches is their dependence upon methods for locating the starting points, which must always be either at the optic nerve or at subsequently detected branch points. Blood vessels were detected by means of mathematical morphology [9]. Matched filters were applied in conjunction with other techniques such as genetic algorithms and piecewise thresholding [10]. The rest of the article are described as follows, the related work is presented in section 2, proposed haemorrhage detection method is presented in section 3, the experimental results are presented in section 4 and the conclusion in section 5.

Related Work: An automatic Binary Mask is a technique used to analyze the end results of the required channels as explained by Hashim *et al*. [11]. Diabetes Retinopathy takes place as the whole retina gets affected. It also affects the whole eye sight. For this type of technique which yields precise result digital imaging is used. The rating cost of the screening process is decreased with retinopathy detection[12]. Color images were used by Zhang *et al*. [14] in order to identify the diabetics. In this study, Non- Invasive approach is mainly used. With the help of Diabetic Retinopathy and the color, notable features, Tongue Segmentation is recorded cautiously and different images for Tongue are demonstrated. No proliferative Diabetic Retinopathy is applied to the tongue effectively.

A good arrangement in the position of the image is provided by the online optic disc detection method. In order to detect the optic disc, adaptive Morphological technique is used. In this study, Cascade classifier method is proposed. It detects both face and eye. The detection performance accomplished is 94.4% as the author implemented with OpenCv with C++ [15]. Diabetic Retinopathy (DR) Detection is done with the help of Image processing technique as expounded by Patil and Chaudhari [16]. The color fundus photographs images detect hemorrhages and micro- aneurysms, hard exudates and cotton-wool spots with the image enhancement technique. The Digital Image Processing technique (DIP) engages the alteration of digital data. The clarity of the image, sharpness and noise reduction can be accomplished with this method. Region of interest is also measured here. Upcoming detecting works can be calculated by Retinopathy Online Challenge. Cross-section analysis can be done with the use of image processing technique. Before the segmentation process color normalization to perform the difference in the respective colors and satisfy it. For the correction, Contrast-Limited Adaptive Histogram equalization is usually applied to the fundus image and it also composes contrast in that particular image. In order to compete that component of vessel to be removed in a green channel image morphological filters are used.

Proposed Method for Hemorrhages Detection: This paper proposes a new supervised approach for Hemorrhages detection based on a NN for pixel classification. The essential feature vector is computed from preprocessed retinal images in the neighborhood of the pixel under consideration. The following process stages may be identified: 1) original fundus image pre-processing for gray-level homogenization and blood vessel enhancement, 2) feature extraction for pixel numerical representation, 3) application of a classifier to label the pixel as vessel or nonvessel and 4) post-processing for filling pixel gaps in detected blood vessels and removing falsely-detected secluded vessel pixels. Input images are

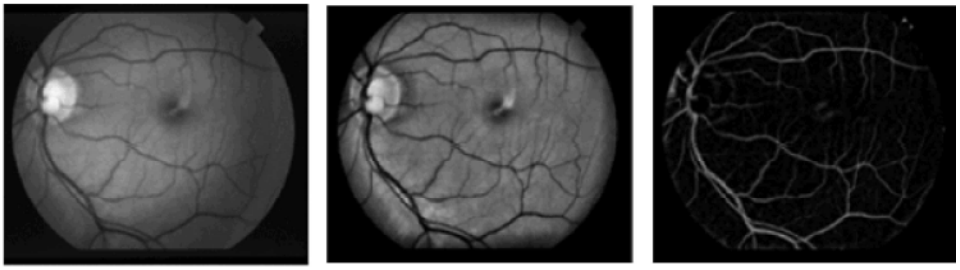

(a) (b) (c)

Fig. 1: Illustration of the preprocessing process: (a) Green channel of the original image. (b) (b) Homogenized image. (c) Vessel-enhanced image.

monochrome and obtained by extracting the green band from original RGB retinal images. The green channel provides the best vessel-background contrast of the RGB-representation, while the red channel is the brightest color channel and has low contrast and the blue one offers poor dynamic range. Thus, blood containing elements in the retinal layer (such as vessels) are best represented and reach higher contrast in the green channel.

Preprocessing: Color fundus images often show imperative lighting variations, poor contrast and noise. In order to reduce these imperfections and generate images more suitable for extracting the pixel features demanded in the classification step, a preprocessing comprising the following steps is applied: 1) vessel central light reflex removal, 2) background homogenization and 3) vessel enhancement. Next, a description of the procedure, illustrated through its application to a STARE database fundus image (Fig. 1), is detailed.

Color fundus images often show important lighting variations, poor contrast and noise. In order to decrease these imperfections and generate images more suitable for extracting the pixel features demanded in the classification step, a pre- processing comprising the following steps is applied: 1) vessel central light reflex removal, 2) background homogenization and 3) vessel enhancement.

Vessel Central Light Reflex Removal: Since retinal blood vessels have lesser reflectance when compared to other retinal surfaces, they appear darker than the background. Although the typical vessel cross-sectional gray-level profile can be approximated by a Gaussian shaped curve (inner vessel pixels are darker than the outermost ones), some blood vessels include a light streak (known as a light reflex) which runs down the central length of the blood vessel. To remove this brighter strip, the green plane of the image is filtered by applying a morphological opening using a three-pixel diameter disc, defined in a square grid by using eight connexity, as structuring element. Disc diameter was fixed to the probable minimum value to reduce the risk of merging close vessels.

Background Homogenization: Fundus images often contain background intensity variation due to nonuniform illumination. Consequently, background pixels may have different intensity for the same image and, even though their gray-levels are usually higher than those of vessel pixels (in relation to green channel images), the intensity values of some background pixels is equivalent to that of brighter vessel pixels. Since the feature vector used to represent a pixel in the classification stage is formed by gray-scale values, this effect may worsen the performance of the vessel segmentation methodology. With the purpose of removing these background lightening variations, a shade-corrected image is accomplished from a background estimate. This image is the result of a filtering operation with a large arithmetic mean kernel.

Vessel Enhancement: The final pre-processing step consists on generating a new vessel-enhanced image, Vessel enhancement is performed by estimating the complementary image of the homogenized image and subsequently applying the morphological Top-Hat transformation. The pre-processing results of two images with different illumination condition are shown in Figure 2.

Feature Extraction: The aim of the feature extraction stage is pixel characterization by means of a feature vector, a pixel representation in terms of some quantifiable measurements which may be easily used in the classification stage to decide whether pixels belong to a real blood vessel or not. A simple breadth-first search algorithm is applied for the calculation of grayscale morphological reconstruction. Pixels of the image are processed sequentially and compared to their

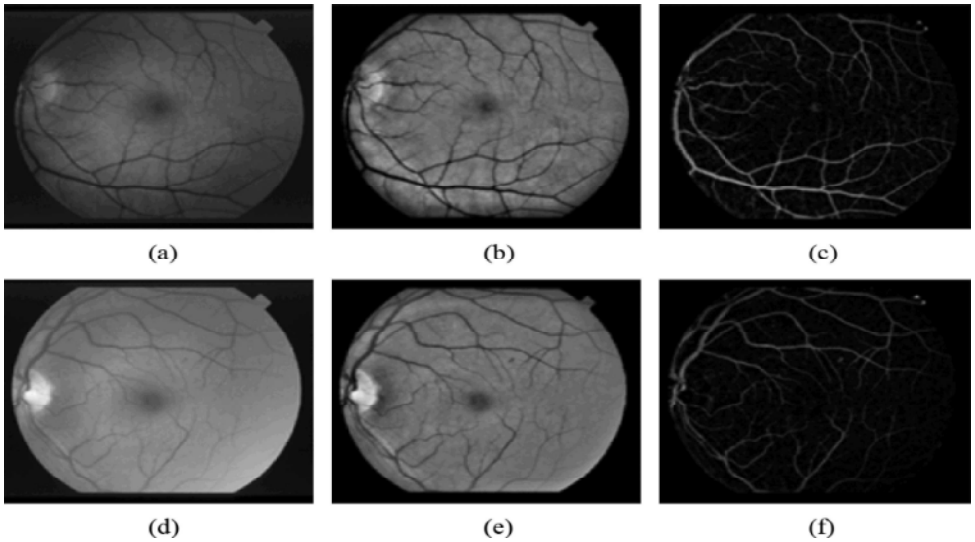

Fig. 2: Pre-processing results of two images with different illumination conditions. (a), (d) Green channel of the original images. (b), (e) Homogenized images. (c), (f) Vessel-enhanced images.

8-neighbors. If all neighbours have a lower intensity, then the pixel itself is a LMR. If there is a neighbouring pixel with higher intensity, then the current pixel may not be a maximum. Pixels of a LMR are considered individually as possible candidates and the pixel with the maximum final score will represent the region; this procedure is referred to as non maximum suppression.

To examine the surrounding of a single maximum pixel in a MA candidate region, the intensity values along discrete line segments of different orientations, whose central pixel is the candidate pixel, are recorded. In this way, a set of cross-sectional intensity profiles is obtained. On the obtained cross-section profiles a peak detection Step is performed. Our aim is to decide whether a peak is present at the center of the profile, i.e., at the location of the candidate point for a specific direction. Several properties of the peak are calculated and the final feature set consists of a set of statistical measures that show how these values vary as the orientation of the cross-section is changing. This way, the variation of important characteristics, such as symmetry and shape of the structure and its difference from the background may be numerically expressed.

The basis of the peak detection method applied is to locate strictly monotonic segments (ramps) of the profile.

Let P denote a profile and P[i] its ith value. A ramp is defined as a segment of the profile, i.e.,P[m],P[m+1],…P[n]

where the sign of the difference between the consecutive values is nonzero and the same along the segment, i.e.,sgn(P[i]-P[i-1])=sgn(P[i+1]-P[i])for every m<i<n.

Additionally, the absolute difference between consecutive values should not be less than parameter min diff and the height of the ramp, i.e., the absolute difference between the first and last value should be not less than parameter min height, either. The value of min diff acts as a lower threshold for the slope of the ramps and it control show sharp the intensity transition should be. The purpose of the min height parameter is to give a lower noise threshold. Based on whether sgn(P[i+1]-P[i]) is positive or negative, the ramps are considered to be increasing or decreasing ramps, respectively. The cross-section profiles of several MAs are examined and found that by setting min diff to 2 and the min height to 3, small monotonic segments that are clearly noise artifacts can be eliminated. After the cross-sectional scanning and peak detection steps are performed for every scan direction on a given candidate, several statistical measures of the resulting directional peak properties are calculated. The increasing-and decreasing ramp height values are stored in the RHEIGHTS set, likewise, the ramp slope values are stored in RSLOPES. The TWIDTHS, PWIDTHS and PHEIGHTS sets contain the top width, peak width and peak height values, respectively.

Let μt, σt and CVt denote the respective mean, standard deviation and coefficient of variation of the values in set T, where the coefficient of variation is the ratio of the standard deviation and the mean, i.e.,

$CV = \sigma/\mu$.

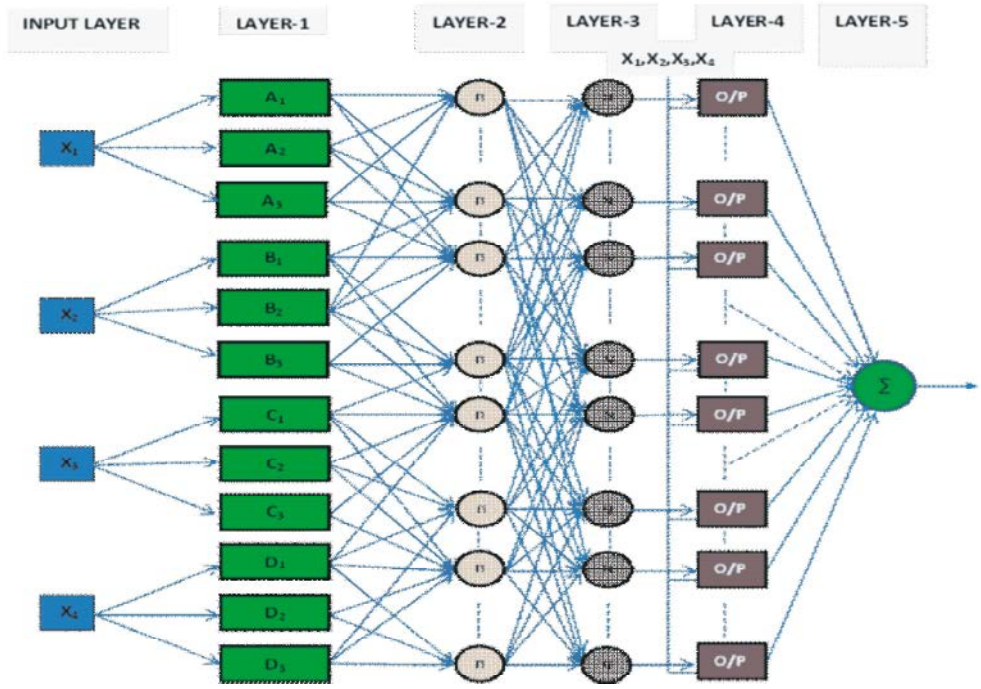

Fig. 3: Schematic diagram for ANFIS structure

The following feature set for classification is considered for classification.

F={μWIDTHS,σPWIDTHS,μTWIDTHS.σTWIDTHS,σRSLOPES,cvRHEIGHTS,cvpHEIGHTS}

Classification Using ANFIS: ANFIS is one of hybrid intelligent neuro-fuzzy inference systems and it functioning under Takagi-Sugeno-type fuzzy inference system. As for the prediction of steering angle for mobile robot we assume the fuzzy inference system under consideration of four inputs i.e Front obstacle distance (X_1), Right obstacle distance (X_2), Left obstacle distance (X_3), target angle (X_4) which are collected from sensors and each input variable has three membership functions(MF) A_1,A_2 and $A_3$$B_1$,$B_2$ and B_3 C_1,C_2 and C_3 and D_1,D_2 and D_3 respectively, then a Takagi-Sugeno-type fuzzyinference system if-then rules is set up as

Rule: if X_1 is A_i and X_2 is B_i and X_3 is C_i and X_4 is D_i then

$$f_n = p_n X_1 + q_n X_2 + r_n X_3 + s_n X_4 + u_n$$

where
i = 1,2,3 and p_n,q_n,r_n,s_n, and u_n are the linear parameters of function f_n.

The function of each layer in ANFIS is discussed as follows;

Input Layer: In this layer, nodes simply pass the incoming signal to layer 1. That is

$$O_{D_i LOD} = X_3$$
$$O_{D_i TA} = X_4$$

First Layer: This layer is the fuzzification layer. Neurons in this layer complete fuzzification process. Every node in this layers an adaptive node and computing the membership function value. The output of nodes in this layer are presented as

$$o_{1,i} = \mu_{A_1}(X_1)$$
$$o_{1,l} = \mu_{C_1}(X_3)$$
$$o_{1,l} = \mu_{D_1}(X_4)$$

Here $o_{1,i}$ is the membership grade of a fuzzy set $S(A_i, B_i, C_i \text{and } D_i)$ and it computing the degree to which the given inputs satisfies the quantifier S. Membership functions defined as follows;

$$\mu_{A_1}(X_1) = \frac{1}{1 + \left[\left(\frac{X_1 - c_1}{a_i}\right)^2\right]^{b_1}}$$

$$\mu_{\exists_i}(x) = \frac{1}{1+\left[\left(\frac{X_2 - c_i}{b_i}\right)^2\right]^{bi}}$$

$$\mu_{C_1}(x) = \frac{1}{1+\left[\left(\frac{X_3 - c_1}{a_1}\right)^2\right]^{b}}$$

$$\mu_{D_i}(x) = \frac{1}{1+\left[\left(\frac{X_4 - c_i}{a_1}\right)^2\right]^{b_i}}$$

a_i, b_i and c_i are parameters that control the centre, width andslope of the Bell-shaped function of node 'i' respectively. Theare also known as premise parameters.

Second Layer: It is also known as rule layer. Every node in this layer is a fixed node and labeled as π_n. Each node in this layer corresponds to a single Sugeno-Takagi fuzzy rule. A rule nodereceives inputs from the respective nodes of layer-2 and determines the firing strength of the rule it represents.

Output from each node is the product of all incoming signals.

$$o_{2,n} = w_n = \mu_{A_i}(X_1), \mu_{B_i}(X_2), \mu_{C_i}(X_3), \mu_{D_i}(X_4)$$

i= 1,2,3 Where w_n represents the firing strength or the truth value, of n rule and n^{th} = 1,2,3…….81 is the number of Sugeno-Takaguzzy rules.

Third Layer: It is the normalization layer. Every node in thiayer is a fixed node and labeled as N_n. Each node in this layer receives inputs from all nodes in the fuzzy rule layer and determines the normalized firing strength of a given rule. The normalized firing strength of the nth node of the n^{th} rule's firing strength to sum of all rules's firing strength.

$$o_{3,n} = \bar{w}_n = \frac{w_n}{\sum_{n=1}^{81} w_n}$$

The number of nodes in this layer is the same the number of nodes in the previous layer that is 81 nodes. The output of this layer is called normalized firing strength.

Fourth Layer: Every node in this layer is an adaptive node.Each node in this layer is connected to the corresponding normalization node and also receives initial inputs X_1,X_2,X_3 and X_4. A defuzzification node determines the weighted consequent value of a given rule define as,

$$o_{4,n} = \bar{w}_n f_n = \bar{w}_n\left[p_n(X_1) + q_n(X_2) + r_n(X_3) + s_n(X_4) + u_n\right]$$

where $\bar{w}_n$ is a normalized firing strength from layer-3 and $[p_n, q_n, r_n, s_n, u_n]$ are the parameters set of this node. These parameters are also called consequent parameters.

Fifth Layer: It is represented by a single summation node. This single node is a fixed node and labeled as ?. This node determines the sum of outputs of all defuzzification nodes and gives the overall system output.

$$o_{5,1} = \sum_{n=1}^{81} \bar{w} f_n = \frac{\sum_{n=1}^{81} w_n f_n}{\sum_{n=1}^{81} w_n}$$

ANFIS Classifier: Gradient descent and Backpropagation algorithms are used to adjust the parameters of membership functions (fuzzy sets) and the weights of defuzzification (neural networks) for fuzzy neural networks. ANFIS applies two techniques in updating parameters. The ANFIS is a FIS implemented in the framework of an adaptive fuzzy neural network. It combines the explicit knowledge representation of a FIS with the learning power of ANNs. The objective of ANFIS is to integrate the best features of fuzzy systems and neural network.

A neuro-fuzzy(ANFIS) classifier is used to detect the abnormalities in the MRI brain images [12]. Generally the input layer consist of seven neurons corresponding to the seven features. The output layer consist of one neuron indicating whether the MRI is of a normal brain or abnormal and the hidden layer changes according to the number of rules that give best recognition rate for each group of features. Here the neuro-fuzzy classifier used is based on the ANFIS technique. An ANFIS system is a combination of neural network and fuzzy systems in which that neural network is used to determine the parameters of fuzzy system. ANFIS largely removes the requirement for manual optimization of parameters of fuzzy system.The neuro-fuzzy system with the learning capabilities of neural network and with the advantages of the rule-base fuzzy system can improve the performance significantly and neuro-fuzzy system can also provide a mechanism to incorporate past observations into the classification process. In neural network the training

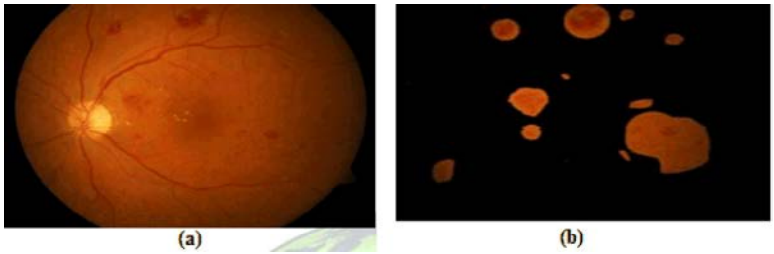

Fig. 4: (a) Fundus Image (b) Hemorrhage Obtained

Table 1: Performance Results On Drive Database Images

Image	Sensitivity	Specificity	PPV	NPV	Accuracy
1	59.97	98.44	82.45	95.27	94.25
2	87.81	96.75	76.03	98.54	95.81
3	77.96	97.70	82.46	96.97	95.30
4	77.65	97.87	83.74	96.87	95.37
5	69.10	98.50	85.98	95.99	95.04
6	68.02	98.25	86.39	94.97	94.02
7	70.39	98.82	89.26	95.99	95.34
8	58.40	99.61	91.72	96.98	96.75
9	67.76	98.72	76.94	97.99	96.89
10	69.44	98.19	82.27	96.59	95.26

Table 2: Performance Results on Stare Database Images

Image	Sensitivity	Specificity	PPV	NPV	Accuracy
1	81.09	97.24	76.01	97.95	98.67
2	87.81	96.75	76.03	98.54	95.81
3	77.96	97.70	82.46	96.97	95.30
4	77.65	97.87	83.74	96.87	95.37
5	69.10	98.50	85.98	95.99	95.04
6	68.02	98.25	86.39	94.97	94.02
7	70.39	98.82	89.24	95.99	95.34
8	58.40	99.61	91.72	96.98	96.75
9	67.76	98.72	76.94	97.99	96.89
10	62.25	97.63	72.45	96.27	94.41

essentially builds the system. However, using a neuro-fuzzy technique,the system is built by fuzzy logic definitions and it is then refined with the help of neural network training algorithms.

Experimental Results

Performance Measures: In order to quantify the algorithmic performance of the proposed method on a fundus image, the resulting segmentation is compared to its corresponding gold-standard image. This image is obtained by manual creation of a vessel mask in which all vessel pixels are set to one and all nonvessel pixels are set to zero. Thus, automated vessel segmentation performance can be assessed. In this paper, our algorithm was evaluated in terms of Sensitivity, Specificity, Positive Predictive Value(PPV), Negative Predictive Value(NPV) and Accuracy [17]. It is defined as follows

$$\text{Sensitivity} = TP/(TP + FN)$$
$$\text{Specificity} = TN/(TN + FP)$$
$$PPV = TP/(TP + FP)$$
$$NPV = TN/(TN + FN)$$
$$\text{Accuracy} = (TN + TP)/(TN + TP + FN + FP)$$

Sensitivity and specificity metrics are the ratio of well-classified vessel and nonvessel pixels, respectively. Positive predictive value is the ratio of pixels classified as vessel pixel that are correctly classified. Negative predictive value is the ratio of pixels classified as background pixel that are correctly classified. Finally, accuracy is a global measure providing the ratio of total well-classified pixels. The segmentation results of proposed method in hemorrhages is given in Fig. 4.

Proposed Method Evaluation: This method was evaluated on DRIVE and STARE database images with available gold-standard images. Since the images' dark background outside the FOV is easily detected. Sensitivity, specificity, positive predictive value, negative predictive value and accuracy values were computed for each image considering FOV pixels only. Since FOV masks are not provided for STARE images, they were generated with an approximate diameter of 650 550. The results are listed in Tables II and III.

A vessel was considered thin if its width is lower than 50% of the width of the widest optic disc vessel. Otherwise the vessel is considered non-thin. On the other hand, a FP is considered to be far from a vessel border if the distance from its nearest vessel border pixel in the gold-standard is over two pixels. Otherwise, the FP is considered to be near. Table IV summarizes the results of this study. This table shows the average ratio of FN and FP provided by the segmentation algorithm for the 10 test images in the DRIVE and STARE databases. The average percent of FN and FP corresponding to the different spacial locations considered are also shown. For both databases, the percent of FN produced in non-thin vessel pixels was higher than that in thin vessel pixels.

Fig. 5: Experimental results of DRIVE database

Fig. 6: Experimental results of STARE database

The experimental results of sensitivity, specificity, PPV, NPV and accuracy of DRIVE data base is shown in Figure 5 and STARE data base is shown in Figure 6.

CONCLUSION

The automatic detection of the hemorrhages presents various challenges. The hemorrhages are hard to distinguish from background variations because it typically low contrast. Automatic detection of hemorrhage can be confused by other dark areas in the image such as the blood vessels, fovea and microaneurysms. It have a variable size and often they are so small that can be easily confused with the images noise or microaneurysyms and no standard database that classify hemorrhage by shape. The most false detection is the case when the blood vessels are adjacent or overlapping with hemorrhages. So the effective detection of hemorrhages methodology is needed. The proposed approach comprises feature extraction and classification. The benefit of the system is to assist the physician to make the final decision without uncertainty. Our proposed hemorrhage segmentation technique does not require any user intervention and has consistent performance in both normal and abnormal images. The proposed hemorrhage detection algorithm produces more than 96% of segmentation accuracy in both publically available DRIVE and STARE Database.

REFERENCES

1. Doi, K., 2007. Computer-aided diagnosis in medical imaging: Historical review, current status and future potential. Computerized Medical Imaging and Graphics, 31: 198-211.
2. Ronald, P.C. and T.K. Peng, 2003 A Textbook of Clinical Ophthalmology: A Practical Guide to Disorders of the Eyes and Their Management, 3rd ed., World Scientific Publishing Company, Singapore.
3. Sukkaew, L., B. Makhanov, S. Barman and S. Panguthipong, 2008.Automatic tortuosity-based retinopathy of prematurity screening system. IEICE transac- tions on information and systems 12.
4. Koreen, S., R. Gelman and M. Martinez-Perez, 2007. Evaluation of a computer-based system for plus disease diagnosis in retinopathy of prematurity. Ophthalmology 114(12): e59-e67.

5. Vickerman, M., P. Keith, Mckay and T. Vesgen, 2009. 2d: Automated, user-interactive software for quantification and mapping of angiogenic and lymphangiogenic trees and networks. The Anatomical Record, pp: 292.
6. Leandro, J.J.G. and R.M. Cesar Jr., 2001. Blood vessels segmentation in retina: Preliminary assessment of the mathematical morphology & the wavelet transform techniques. Proceding on Computer Graphics and Image Processing, pp: 84-90.
7. Tolias, Y.A. and S.M. Panas, 1998. A fuzzy vessel tracking algorithm for retinal images based on fuzzy clustering. IEEE Trans Med Imaging, 17: 263-273.
8. Zana, F. and J.C. Kelin, 2001. Segmentation of vessel-like patterns using mathematical morphology and curvature evaluation. IEEE Trans on Image Process, 10: 1010-1019.
9. Al-Rawi, M. and H. Karajeh, 2007. Genetic algorithm matched filter optimization for automated detection of blood vessels from digital retinal images. Compute Methods Programs Boomed, 87: 248-253.
10. Hashim, F.A., N.M. Salem and A.F. Seddik, 2013. Preprocessing of color retinal fundus images. Proceeding of the 2nd International Japan-Egypt Conference on Electronics, Communications and Computers (JEC-ECC), pp: 258-261.
11. Faust, O., A.U. Rajendra, E.Y.K. Ng, K.H. Ng and J.S. Suri, 2012. Algorithms for the automated detection of diabetic retinopathy using digital fundus images: A review. J. Med. Syst., 36(1).
12. Akara, S., U. Bunyarit and B. Sarah, 2008. Automatic exudates detection from non-dilated diabetic retinopathy retinal images using fuzzy C-means clustering. Comput. Med. Imag. Grap., 32: 720-727.
13. Zhang, B., B.V. Kumar and D. Zhang, 2014. Detecting diabetes mellitus and nonproliferative diabetic retinopathy using tongue color, texture and geometry features. IEEE T. Bio-Med. Eng., 61(2): 491-501.
14. Claudio, A.P., A.S. Daniel, C.M. Aravena, C.I. Perez and T.J. Verdaguer, 2013. A new method for online retinal optic-disc detection based on cascade classifiers. Proceeding of the IEEE International Conference on Systems, Man and Cybernetics (SMC, 2013), pp: 4300-4304.
15. Patil, J.D. and A.L. Chaudhari, 2012. Tool for the detection of diabetic retinopathy using image enhancement method in DIP. Int. J. Appl. Inform. Syst., 3(3).
16. Wen, Z., Z. Nancy and W. Ning, 2010. Sensitivity, specificity, accuracy, associated confidence interval and ROC analysis with practical SAS implementations. Proceeding of the SAS Conference. Baltimore, Maryland, pp: 9.